GA–A26744

# MEASUREMENTS OF THE INTERNAL MAGNETIC FIELD USING THE B-STARK MOTIONAL STARK EFFECT DIAGNOSTIC ON DIII-D

by
N.A. PABLANT, K.H. BURRELL, R.J. GROEBNER,
C.T. HOLCOMB and D.H. KAPLAN

JUNE 2010

GENERAL ATOMICS

# DISCLAIMER

GA–A26744

# MEASUREMENTS OF THE INTERNAL MAGNETIC FIELD USING THE B-STARK MOTIONAL STARK EFFECT DIAGNOSTIC ON DIII-D

by
N.A. PABLANT,* K.H. BURRELL, R.J. GROEBNER,
C.T. HOLCOMB† and D.H. KAPLAN

This is a preprint of a paper to be presented at the 18th Topical Conference on High Temperature Plasma Diagnostics, May 16–20, 2010 in Wildwood, New Jersey and to be published in Review of Scientific Instruments.

*University of California-San Diego, La Jolla, California USA
†Lawrence Livermore National Laboratory, Livermore, California USA

Work supported in part by
the U.S. Department of Energy
under DE-FC02-04ER54698, DE-FG02-07ER54917
and DE-AC52-07ER27344

GENERAL ATOMICS ATOMICS PROJECT 30200
JUNE 2010

## ABSTRACT

Results are presented from the B-Stark diagnostic installed on the DIII-D tokamak. This diagnostic provides measurements of the magnitude and direction of the internal magnetic field. The B-Stark system is a version of a motional Stark effect (MSE) diagnostic based on the relative line intensities and spacing of the Stark split $D_\alpha$ emission from injected neutral beams. This technique may have advantages over MSE polarimetry based diagnostics in future devices, such as ITER. The B-Stark diagnostic technique and calibration procedures are discussed. The system is shown to provide accurate measurements of $B_\theta / B_T$ and $|B|$ over a range of plasma conditions. Measurements have been made with toroidal fields in the range 1.2–2.1 T, plasma currents in the range 0.5–2.0 MA, densities between 1.7–9.0 × $10^{19}$ $m^{-3}$, and neutral beam voltages between 50–81 keV. The viewing direction and polarization dependent transmission properties of the collection optics are found using an *in situ* beam into gas calibration. These results are compared to values found from plasma equilibrium reconstructions (**EFIT**) and the MSE polarimetry system on DIII-D.

# I. INTRODUCTION

Measurements of the internal magnetic field are important for the accurate reconstruction of the plasma equilibrium in tokamaks and stellarators. Diagnostics able to make these types of measurements are considered to be essential in present-day devices and are usually based on motional Stark effect (MSE) polarimetry for measurements of the magnetic pitch angle. Measurements of the direction of the magnetic field provide a strong constraint on the plasma current profile. In addition, while not routinely used, measurements of $|B|$ can provide a strong constraint on the pressure profile.[1,2]

The B-Stark diagnostic, installed on the DIII-D tokamak at General Atomics, is a version of an MSE diagnostic based on the relative line intensities and spacing of the Stark split $D_\alpha$ emission from injected neutral beams. With this system both the magnitude and direction of the internal magnetic field can be measured. In this paper a discussion is given of the theory, calibration and final performance of this system. Measurements of the magnetic field are compared against values found from plasma equilibrium reconstructions (**EFIT**)[3] and the MSE polarimetry[4] system.

The B-Stark diagnostic may have advantages over MSE polarimetry in future devices with high densities and temperatures. Under these conditions, coatings can develop on the plasma facing mirrors that interfere with MSE polarimetry by changing the polarization state of the incident light.[5] In addition, the need for polarization preserving collection optics present a challenge for the design and calibration of an MSE polarimetry system.[6] The B-Stark diagnostic is not sensitive to the polarization direction. While it is sensitive to polarization dependent transmission, there is a simple calibration procedure that can be used to correct for this effect. This calibration is done by filling the vacuum vessel with a low density gas and firing the neutral beam between plasma discharges (beam into gas).

The theory and design of this diagnostic has been described previously along with preliminary results in Ref. 7. Diagnostics to measure the magnetic field line pitch, $B_\theta / B_T$, using the Stark intensities have been developed previously on TEXTOR[8] and JET.[9] Both of these diagnostics had non-optimal midplane viewing geometries which required them to use additional information to determine $B_\theta / B_T$. More recent preliminary results from TEXTOR, using an installation with favorable viewing geometry, have shown promising results.[10] Both the TEXTOR and JET diagnostics have relied on the total $\pi$ and $\sigma$ intensities and have required assumptions about the upper state level populations. Measurements of $|B|$ from the Stark spacing have been made previously at JET[9,11] and in the MST-reversed field pinch.[12]

The B-Stark diagnostic at DIII-D has an optimized viewing direction for measurements of $B_\theta / B_T$ and a spectral resolution sufficient for the individual Stark lines to be fit, removing the need for assumptions about the level populations. In addition DIII-D has an existing MSE polarimetry system with which measurements can be compared.

## II. THEORY

The B-Stark diagnostic relies on the emission spectrum of deuterium atoms from the neutral heating beams on DIII-D. The Stark split emission from the $D_\alpha$ ($n=3\rightarrow n=2$) transition is used, around a wavelength of 6561.0Å. Stark splitting of the energy levels occurs when the atom is exposed to an electric field.

For the deuterium atoms injected into the plasma by the neutral beams, there are two sources of electric fields. There is a Lorentz electric field produced by the particle's motion across the magnetic field, and a radial electric field from the plasma. This electric field can be written as $\mathbf{E}=\mathbf{v_b}\times\mathbf{B}+\mathbf{E_r}$, where $\mathbf{v_b}$ is the velocity of neutral beam atoms and $\mathbf{B}$ is the local magnetic field.

Typical $\mathbf{E_r}$ fields in DIII-D are two orders of magnitude smaller than the Lorentz electric field and can be ignored in the B-Stark calculations. In certain high performance plasmas the $\mathbf{E_r}$ field can become a significant contribution and a calculation including $\mathbf{E_r}$ is needed.[13]

The effect of Zeeman splitting in calculating the spacing between the lines is negligible for the magnetic field strengths at DIII-D, and a linear Stark effect is assumed.[9] For the linear Stark effect the spacing between the lines can be written as $\Delta\lambda=\lambda_0^2\,(3/2)(ea_0/hc)|\mathbf{E}|$.[14]

The Stark lines are polarized parallel to the electric field for $\Delta m=0$ ($\pi$ transitions), and polarized perpendicular to the field for $\Delta m=\pm1$ ($\sigma$ transitions). The intensity of the emission also varies with the angle relative to $\mathbf{E}$, and the intensity ratio of $\pi$ to $\sigma$ light can be used to find the direction of the electric field. In general this requires the populations of the $n=3$ states to be known. Two sets of lines, $\pi\pm3/\sigma\pm1$, originate from the same upper level removing the dependence on the level populations (Fig. 1).[14] The intensity ratio of these lines is

$$\frac{I_{\pi 3}}{I_{\sigma 1}} = \frac{2\sin^2\Theta}{1+\cos^2\Theta}\,AT_f \quad , \tag{1}$$

where $\Theta$ is the angle between the viewing direction and the electric field, $A$ is the constant ratio of the transition probabilities, and $T_f$ is the $\pi$ to $\sigma$ transmission ratio for the collection optics.

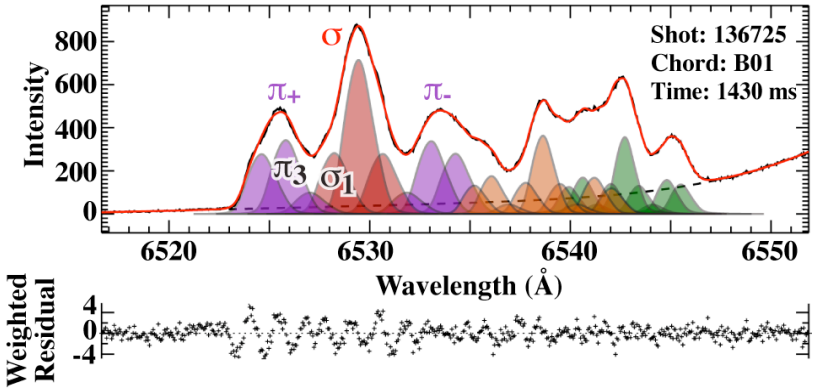


FIG. 1. B-Stark spectral fit at full field, 1.95 T. Shot 136725 at 1.4 s with 10 ms integration time. Data is shown as the solid black line, the fit is shown as a solid red line. The individual Stark lines that make up the spectrum are shown. The $\pi$ and $\sigma$ lines from the full energy beam component are shown in purple and red, respectively. Lines from the half and third energy beam components are shown in orange and green. The dashed black line shows the background model used to take into account fast-ion and main-ion emission.

## III. EXPERIMENTAL SETUP

The sensitivity of the B-Stark diagnostic to changes in the direction of the magnetic field is highly dependent on the viewing direction. From Eq. (1) it can be shown that the optimal viewing angle is 62.1° from the electric field. In DIII-D, where $B_\theta / B_T$ is small, the electric field is near vertical. The B-Stark installation on DIII-D provides two viewing chords with optimized viewing directions and a view of two neutral heating beams as shown in Fig. 2. The viewing locations are at major radii of 191.5 and 205.3 cm and have a radial resolution of 1–3 cm. Additional design considerations and the final experimental setup have been described previously in Ref. 7.

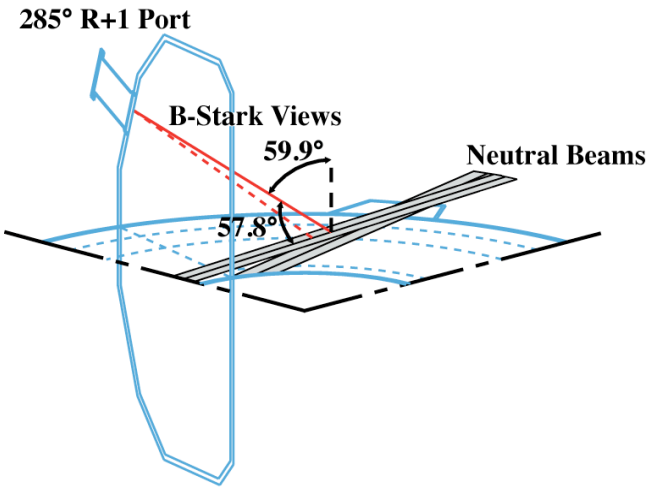


FIG. 2. B-Stark diagnostic geometry. Outlines of the of the DIII-D vessel are shown at the midplane and at a toroidal angle of 285°. The B-Stark viewing chords cross the 330°Left and 330°Right neutral beams. The angle between the 330°Left neutral beam and the B-Stark chord is 57.8°. The angle between the vertical direction and the B-Stark chord is 59.9°. The FWHM of the neutral beams is ~14 cm in the horizontal direction and ~26 cm in the vertical direction.[16] (With permission, adapted from N.A. Pablant et al. Rev. Sci. Instrum. **79**, 10F517 (2008). Copyright 2008, American Institute of Physics.)

The viewing optics are installed with a lens mask in place to limit geometrical Doppler broadening. Collected light is coupled to a Czerny-Turner spectrometer using custom fiber bundles packed into a line at the entrance slit for increased throughput into the spectrometer. The spectrum is recorded using a Sarnoff CAM1M100 charge coupled device (CCD) camera with a 16 $\mu$m pixel pitch. The top and bottom halves of the chip correspond to the two views, and are binned vertically resulting in spectra with 1024 channels. The present configuration has a dispersion of 0.06Å/channel, a spectral range of ~60Å, and an instrumental response with a full width at half maximum (FWHM) of 0.5Å. The present system is an upgrade to the

configuration as described in Ref. 7 and provides a wider spectral range and significantly improved light throughput.

In addition to the views with optimized geometry, four chords from the midplane charge exchange recombination (CER) system were tuned to $D_\alpha$ for the dedicated experiment described in Section VI. These midplane views are not sensitive to the magnetic pitch angle, but provide excellent data for measurements of $|B|$. The configuration of this system is described in Ref. 15. In order to use the system for measurements of $|B|$ the entrance slits on the spectrometer were reduced to 70 $\mu$m. In this configuration the system has an instrumental response with a FWHM of ~1Å and a dispersion of 0.10Å/channel.

## IV. SPECTRAL FITTING

To extract the magnitude and direction of the magnetic field a model is fit to the Stark split $D_\alpha$ spectrum. Spectral fitting is done using a modified version of the non-linear least squares fitting package, **CERFIT**.[17]

The DIII-D neutral beams inject particles primarily at three energies, the full, half and third energy beam components. Each of these energy components produce emission with a different Doppler shift and Stark splitting (see Figs. 1 and 3). All three components are included in the B-Stark spectral model.

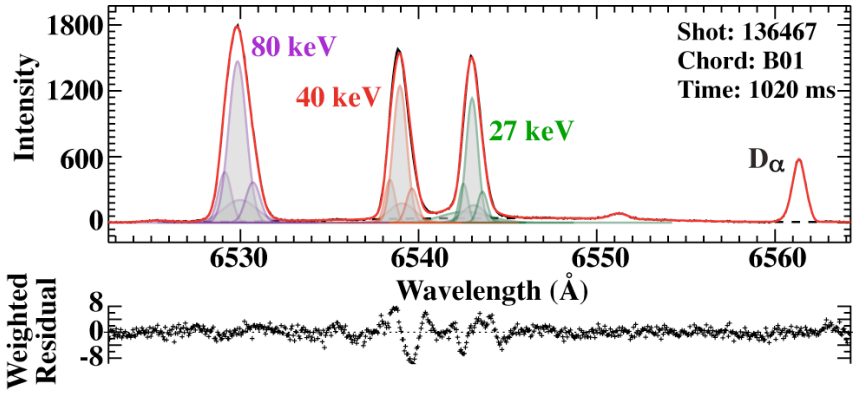


FIG. 3. Spectrum from a deuterium beam into helium gas shot with no magnetic field. The gas pressure used was 0.37 mTorr. The unshifted $D_\alpha$ peak is from residual $D_2$ gas in the vessel. The profile for the full energy beam emission has been fit using four Gaussians, outlined in purple. This profile was then scaled to fit the half (orange) and third (green) emission. A single Gaussian was used for the emission between the half and third components and attributed to the third component profile. Shot 136467, 30 ms integration time.

The line spacing is assumed to be described by the linear Stark effect. The fit variables in the spectral model are the upper state level populations, the intensity ratio of the $\pi$ versus $\sigma$ lines [see Eq. (1)], the beam velocity projected onto the viewing direction, the effective electric field, and the spectrometer fiducial (central wavelength). Each of the beam components is allowed to have unique upper state populations. The background emission is described using Gaussians and up to a quadratic polynomial. A typical fit using this model has 27 free parameters.

The lines from each beam component are given a unique line profile found using a beam into gas calibration as described in Section V.A. It is assumed that each line within a Stark multiplet has the same profile.

To obtain the best spectra, background subtraction is done by subtracting time slices where the neutral beam is off from those where the beam is on. This process removes any background impurity emission from the resulting spectrum. The spectrum still contains any beam dependent emission including main-ion and fast-ion charge exchange $D_\alpha$ emission. In

general background subtraction is not needed unless impurity emission lines are present in the spectrum. For typical plasma shots at DIII-D a lack of background subtraction has only a minor effect on the B-Stark results. For the fits described in this paper the main-ion and fast-ion emission are modeled using a single Gaussian and a linear background term. This background model is shown in the figures as a dashed black line.

# V. CALIBRATION

Several types of calibrations are needed to accurately fit and analyze the Stark split $D_\alpha$ spectrum. Calibrations are necessary to find the line shape of the emission from the neutral beams, the viewing geometry with respect to the beams, and the transmission properties of the collection optics.

An in-vessel spatial calibration is used to find the radius at which the views cross the neutral beam. This calibration assumes that the location of the neutral beams is known. The calibration is done by aligning a target with the expected beam location then back illuminating B-Stark fibers and measuring the spot location.

The beam emission line profiles are found using the spectrum from a beam into gas shot without magnetic field, as described in Section V.A.

A beam into gas with toroidal magnetic field calibration is used to find the viewing geometry and the relative transmission of $\pi$ to $\sigma$ light though the collection optics. This calibration is discussed in Section V.B.

In addition, a careful calibration of the dispersion and intensity response of the system are necessary in order to make accurate measurements of the line spacing and intensities.

## A. LINE PROFILES

To fit the Stark split $D_\alpha$ spectrum it is necessary to know the shape of each of the beam emission lines. There are a number of effects that contribute to this line profile shape. The primary effects are the spectrometer response, Doppler broadening due to the geometrical divergence of the neutral beam, and Doppler broadening due to the finite size of the collection optics. Additional effects that can contribute to the line profiles are the energy spread of the neutral beam, the change in the magnetic field over the viewing volume, and variations in the beam energy during the integration time. An analytical presentation of some of these effects is given in Ref. 18.

The neutral beams at DIII-D have a divergence of ~0.7° in the horizontal direction and ~2° in the vertical direction.[16] For the B-Stark views, which have a large vertical component, the line width is primarily due to Doppler broadening from the beam divergence. This provides the limit on how well the Stark lines can be resolved. For the CER midplane views described in Section III, which have purely horizontal views, the instrumental width is comparable to the Doppler broadening from the beam divergence and from the finite lens size.

Due to the Doppler broadening effects, the line profile from each of the neutral beam energy components will be different. In addition, the beam divergence will cause each line within the manifold to have a different line shape. This is due tothe change in the Stark line

spacing over the range of angles from the neutral beam. The severity of this last effect is highly dependent on the viewing and magnetic geometry. For the B-Stark views at DIII-D this effect is small, ~4%, and is ignored. For the CER midplane views, this effect causes a change of ~15% in the beam divergence contribution to line width across the Stark manifold. The effect of this 15% variation on the final line shape is significantly lessened due to the wide instrumental response from the spectrometer and is ignored for these chords as well.

For the work described in this paper, an empirical approach is used to determine the beam emission line profiles from a low density beam into gas shot. Without a magnetic field, there is no splitting of the $D_\alpha$ line and three peaks are seen in the spectrum corresponding to the full half and third components of the neutral beam, see Fig. 3. The line profile shape can be approximated by fitting these peaks as a sum of Gaussians. This method of determining the line shape takes into account many of the line broadening effects including the spectrometer response, beam divergence and the finite lens size.

In addition to the emission at wavelengths corresponding to the three beam energies, there is a broad emission between the half and third components. This emission can be seen in Fig. 3 and is due to the break up of triatomic deuterium ions during accelebration, $D_3^+ \rightarrow D_2^+ + D$. To handle this broad emission in the Stark model, an approximation is made by fitting the emission with a single Gaussian and attributing it to the third component profile.

To maintain a consistent definition for the wavelength center of the beam emission, the line profiles for all three beam components are constrained to have the same shape, but are allowed different intensities and widths. For every Gaussian in each profile, the width and the distance from the line center are multiplied by a scale factor. For the current work the line center was chosen to be the centroid of the profile.

While this type of calibration gives a reasonable approximation to the true beam into plasma line profiles, collisions of the neutral beam particles with the background gas effectively increases the beam divergence and produces beam profiles that are too wide to correctly fit the plasma spectra. An assessment of the magnitude of this effect has been made by using different gas species and pressures. A number of beam into gas shots were examined where the vessel was filled with helium, xenon or deuterium gas at various pressures ranging from 0.07 to 0.70 mTorr. Changes in the line width of ~5% were observed with the narrowest profiles found at the lowest pressures.

For the final calibration, helium is used as it does not contain any spectral lines within the $D_\alpha$ spectral range used by the B-Stark diagnostic.

## B. GEOMETRY AND MIRROR PROPERTIES

One of the advantages of the B-Stark diagnostic over MSE is that the necessary geometry and transmission properties can be straightforwardly determined *in-situ* by using a beam into

gas with toroidal field calibration. This type of calibration can be done whenever the properties of the collection optics are expected to have changed.

In order to make measurements of $B_\theta / B_T$ the relative transmission of $\pi$ versus $\sigma$ light through the collection optics must be known. Once the light travels though the fiber optics, the polarization will be scrambled making the relative transmission though the spectrometer unimportant. The simplest way to approximate the relative transmission through the collection optics is to introduce a transmission factor into the calculation of the magnetic pitch angle as shown in Eq. (1). This simplistic treatment is effective in DIII-D where the relative transmission of $\pi$ and $\sigma$ light is fairly similar ($T_f \approx 0.7$) and where the direction of the Lorentz electric field does not vary greatly. For other installations a more complicated treatment may be necessary.

To fully determine the viewing geometry, also required to measure $B_\theta / B_T$, a view of two neutral beams is needed. If the geometry is well known from an in-vessel spatial calibration, the transmission factor can be found using only a single beam. If only $|B|$ is to be measured, then the relevant geometry can be found with a single beam as well.

This beam into gas calibration requires that the magnetic field at the viewing location is known. For the DIII-D installation, where the viewing locations are on the midplane, the vacuum magnetic field is in the toroidal direction and has a $1/R$ dependence on major radius. Accordingly the magnetic field can be found from the toroidal field coil current and the major radius of the viewing location. The beam into gas spectra are fit using the same fitting technique as for plasma spectra, as described in Section IV. The spectral fit provides measurements of the Lorentz electric field, the ratio of the $\pi$ to $\sigma$ emission and the projected beam velocity.

To calculate the geometry, the projection of the viewing direction along the neutral beam is found for two neutral beams using the expression for the Lorentz electric field with a known magnetic field. The two measurements are then related though the known angle between the two beams. From this relation the viewing direction can be derived. Once the geometry and magnetic field direction is known, the transmission factor can be found from Eq. (1).

In practice, if the actual viewing location or wavelengths of the Stark lines are incorrectly determined or the fitting model cannot exactly reproduce the observed spectrum, the beam into gas calibration will return an effective geometry and transmission factor that can be thought of as a set of three calibration coefficients.

The ability to use this calibration technique is unique to the B-Stark diagnostic. For a beam into gas shot, the $n = 3$ level populations are not expected to be in statistical equilibrium. This can readily be seen from the difference in the shape of the Stark spectrum between the beam into plasma and the beam into gas cases in Figs. 1 and 4, respectively. This

does not present a problem for the B-Stark diagnostic because the level populations are free parameters in the fitting model.

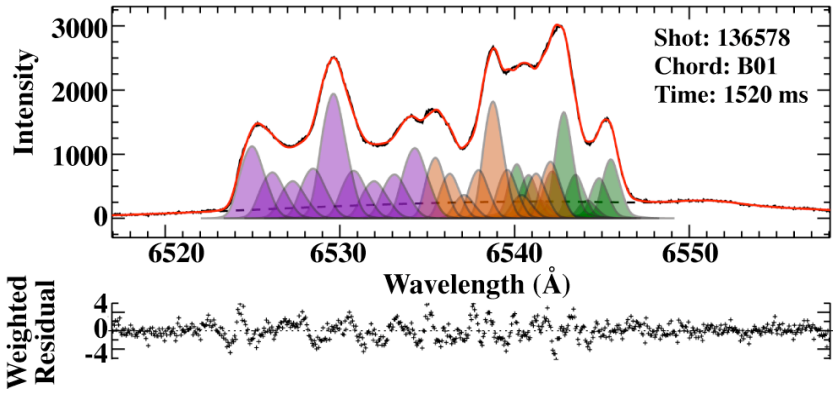


FIG. 4. Spectrum from a beam into helium gas shot with a toroidal magnetic field of 1.9 T. Shot 136578, 240 ms integration time. This longer integration time is needed for the beam into gas calibration as the beam emission intensity is reduced from the beam into plasma case.

## VI. RESULTS

In order to make the best possible comparisons with the MSE polarimetry system over a wide range of conditions, a dedicated experiment was conducted at DIII-D. For this experiment inner wall limited L-mode plasmas were used. This shape was used as it allowed for the widest possible range of densities and currents while using a single plasma shape. In addition it provided a discharge free of edge localized modes (ELMs), simplifying the spectral analysis. Beam timing was optimized to provide good background subtraction for both beams viewable by the B-Stark system, and to provide optimal data for the MSE polarimetry system. A portion of the midplane CER system was tuned to the $D_\alpha$ spectrum to be used for measurements of $|B|$.

Over the course of the experiment measurements were made with toroidal fields in the range 1.2–2.1 T, plasma currents in the range 0.5–2.0 MA, densities between 1.7–9.0 $\times$ $10^{19}$ $m^{-3}$, and neutral beam voltages between 50–81 keV. In addition to this dedicated run day, the B-Stark system has been routinely taking data in its current configuration since March 2009.

Beam into gas shots, both with and without magnetic fields were taken for the calibrations in Section V. These calibrations were done using beam into helium gas discharges with gas pressures of 0.37 mTorr. These calibrations, including the full geometry calibration, were used for all results presented in this paper.

A typical spectral fit for the B-Stark system at a magnetic field of 1.95 T is shown in Fig. 1. Asymmetries in the Stark spectrum are primarily due to the line profiles being asymmetric and not to the intensities of the Stark lines.

Measurements of both $|B|$ and $B_\theta / B_T$ were made with over the entire range of plasma conditions achieved during the dedicated experiment as well as during numerous H-mode shots runfor other experiments, including shots with reversed plasma current. Both measurements were possible even at fields as low as 1.1 T with 80 keV beams, or with beam voltages as low as 50 keV with 2 T magnetic fields. This demonstrates that the B-Stark diagnostic is effective even with poor separation of the Stark lines and without constraints on the level populations. A spectral fit at low field is shown in Fig. 5. Because of the reduced line separation at low fields, the fitter has more flexibility in adjusting the model parameters; this results in reduced residuals while also increasing the uncertainty in the determination of the final model parameters.

A comparison of $B_\theta / B_T$ between the B-Stark measurements and values from an **EFIT** reconstruction with MSE polarimetry is shown in Fig. 6. If the calibration of the transmission factor is manually adjusted by ~4%, an excellent match with **EFIT** can be obtained. This improvement is also illustrated in Fig. 6.

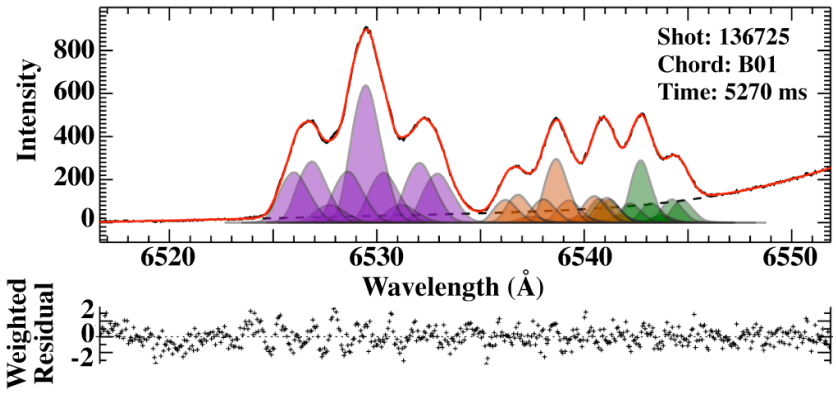


FIG. 5. B-Stark spectral fit at low field, 1.4 T. Shot 136725 at 5.3 s with 10 ms integration time. Even with poor line separation it is possible to determine the pitch angle without assumptions about the level populations.

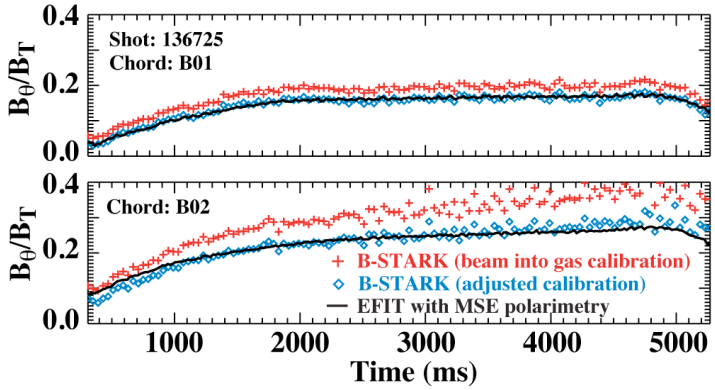


FIG. 6. Comparison of $B_\theta / B_T$ between B-Stark and reconstructions from EFIT with MSE polarimetry. The two B-Stark viewing chords are shown. The toroidal magnetic field is ramped down in this shot with values on axis decreasing from 2.15 T to 1.5 T, as shown in Fig. 7. B-Stark measurements, calibrated using an *in situ* beam into gas calibration (red crosses), are made using a 10 ms integration time. EFIT with MSE polarimetry results (solid line) are calculated every 20 ms with a 10 ms averaging used for the MSE polarimetry measurements. For both views an adjustment in the value of the transmission factor by ~4% produces an good match with the EFIT values, as shown in blue diamonds. The scatter of the measurements at the end of the shot is due to the low magnetic field.

Unlike $B_\theta / B_T$, the value of $|B|$ found from an **EFIT** reconstruction with MSE polarimetry is not a well constrained quantity. For a more accurate reconstruction of $|B|$ a kinetic **EFIT** must be run which uses fitted electron and ion temperature and density profiles as well a calculated fast-ion distribution. These additional parameters serve to constrain the kinetic pressure profile.[1,3] A comparison of $|B|$ between the B-Stark system, including the midplane CER views, and a kinetic **EFIT** is shown in Fig. 7.

Another way to examine the accuracy of the $|B|$ measurement is to compare measurements between the B-Stark and midplane CER views. These two systems have

different views and instrumental responses, producing a large difference in the beam emission profiles. In addition the systems have entirely different light collection optics, spectrometers and camera systems. The viewing radius of one of the CER views coincides with one of the B-Stark views providing a simple comparison between the two systems. These two views produce a measurement of $|B|$ that matches to better than 0.005 T for all shots that have been analyzed (Fig. 7).

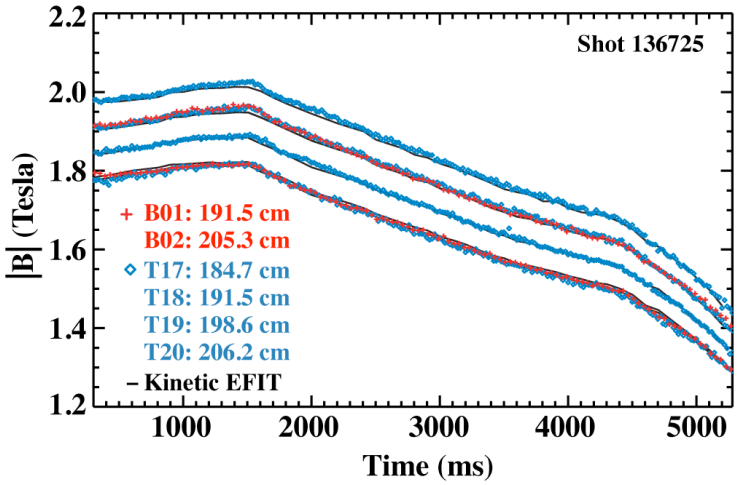


FIG. 7. Comparison between B-Stark and kinetic EFIT values for $|B|$. Measurements from the B-Stark views (**B01**, **B02**) are shown as red crosses. The midplane CER views (**T17–T20**) are included and shown as blue diamonds. **EFIT** values are shown with solid black lines. For the B-Stark measurements of $|B|$, values of $B_\theta / B_T$ found from **EFIT** are used in determining the angle between the beam and the magnetic field. The values for chords **B01** and **T18** view the plasma at the same radii and the measurements overlap, the same is true for **B02** and **T20**.

To examine the performance of the B-Stark system it is important to look at both the random and systematic errors. Random errors are due to photon noise; the amount that this affects the measured parameters depends on the uniqueness of the fitting solution. The highest accuracies are found when the beam emission intensity and Stark line spacing are maximized. This is achieved at lower plasma densities with full magnetic field and maximum neutral beam voltage.

For the B-Stark system the two main sources of systematic error are the determination of line profile shapes and the choice of background model used for spectral fitting. Both the analysis of plasma shots as well as the calibration of the geometry and transmission factor are affected. Errors in the line profiles or the background models ultimately cause a mismatch between the model and the actual spectra and are reflected in the residuals seen in Figs. 1, 4 and 5. When examining multiple times from a single shot, or shots with similar plasma conditions, the fitting errors will be the same in every case, producing a systematic offset in the measurements from the true values.

Because the spectra from beam into gas shots are much different than those from plasma shots, fitting errors become a significant issue for an accurate *in situ* beam into gas calibration of the viewing direction and the transmission factor. Even small errors in the determination of the profiles or the background can lead to significant calibration errors.

Measurements of $|B|$ were made with high accuracy over the entire range of plasma conditions, including at low fields. With 10 ms integration time, the random errors in the measurement of $|B|$ are 0.001–0.002 T for the B-Stark views and 0.002–0.004 T for the midplane CER views. The higher errors for the CER views are due to the lower light throughput of that system. These values are found by looking at the standard deviation in the measurements over periods where $|B|$ is constant or changing linearly. This may be an overestimation of the error due to actual variations in the magnetic field. The systematic error in measurements of $|B|$ is estimated to be less than ~0.005 T.

At full field the random error in measuring the ratio of the $\pi \pm 3$ to $\sigma \pm 1$ lines is ~0.5% for the B-Stark chords and ~1.5% for the CER midplane chords. How this error translates into the error in $B_\theta / B_T$ depends on the exact viewing geometry. For the two B-Stark viewing chords the errors in $B_\theta / B_T$ are ~0.004 (0.2°) and ~0.006 (0.3°). This error in the pitch angle is comparable to the error in the measurements from MSE polarimetry system.[19] The error in the pitch angle becomes larger with lower emission intensity or reduced Stark line separation.

Using a *in situ* beam into gas calibration without any adjustment, the current systematic error in determining $B_\theta / B_T$, as compared to **EFIT** with MSE polarimetry, can be as large as 0.05 (3.0°) and depends on the choice of profile shape and background model. This systematic error can be resolved by a ~5% adjustment of the geometry or transmission factor. In addition, the systematic difference between B-Stark and **EFIT** varies with density. For the density range achieved in the dedicated experiment a change in the comparison of $B_\theta / B_T$ of 0.02 (1°) is seen. This systematic change with density is thought to be primarily caused by fast ion emission, which is not accurately handled in the current model. The intensity of the fast-ion emission falls off with increasing density, producing this effect. Work is continuing to resolve these calibration issues through the inclusion of fast-ion model for the background and better techniques for the determination of the line profiles.

## VII. CONCLUSION

The B-Stark diagnostic technique has been shown to be effective for making measurements of the magnitude and direction of the internal magnetic field in the DIII-D tokamak. Both measurements have been shown to be possible with high precision over the range of plasma parameters accessible in this device. These measurements are possible even at low fields or beam energies where the individual Stark lines are not well resolved. With the current installation, measurements of $B_\theta / B_T$ can be made with a time resolution and measurement precision comparable to MSE polarimetry. Measurements of $|B|$ are highly accurate and would provide a strong constraint for magnetic reconstruction, particularly for the pressure profile.

The beam emission line profiles, needed in order to fit the Stark spectrum, can be reasonably approximated through the use of a beam into gas shot without magnetic field. Scattering of the neutral beam particles on the background gas broadens the emission profile. This effect is minimized though the use of a low gas pressure.

The geometry of the views as well as the necessary transmission properties of the first mirror and collecting optics can be calibrated using a beam into gas shot. This calibration relies on the ability to measure the $\pi$ to $\sigma$ intensity ratio without assumptions about the level populations. The use of this calibration is promising for use of this system in future devices where coatings on the plasma facing mirrors may change the reflection properties. Improvements in the calibration are still needed for accurate measurements of $B_\theta / B_T$. This is likely achievable though better determination of the line profiles and improvements in modeling of the background emission. The calibration of the geometry needed for measurements of $|B|$ has been shown to be highly accurate.

The precision of the B-Stark diagnostic is dependent on both the light throughput and on the separation of the Stark lines. The precision of the current installation on DIII-D has room for significant improvement through the use of a faster spectrometer. The use of an atomic physics model to calculate the level populations would also provide an improvement in the diagnostic precision. The use of such an atomic code can greatly improve the precision in the determination of $B_\theta / B_T$ by allowing the total $\pi$ versus $\sigma$ intensity to be used. At lower magnetic fields or beam energies, where the individual Stark lines cannot be resolved, a calculation of level populations becomes necessary. At low enough fields the linear Stark approximation becomes invalid and a more complicated model of the Stark emission becomes necessary.

Overall the B-Stark diagnostic has been shown to be an effective alternative to MSE polarimetry in current and future fusion devices. In devices with stronger magnetic fields and higher energy beams, such as ITER, the spacing between the Stark lines will be larger, and improved measurement accuracy is expected.

## REFERENCES

[1]L. Zakharov, E. Foley, F. Levinton, and H. Yuh, Plasma Phys. Rep. **34**, 173 (2008).

[2]E. L. Foley, F. M. Levinton, H. Y. Yuh, and L. E. Zakharov, Rev. Sci. Instrum. **79**, 10F521 (2008).

[3]L. L. Lao, H. E. St. John, Q. Peng, J. R. Ferron, E. J. Strait, T. S. Taylor, W. H. Meyer, C. Zhang, K. I. You, Fusion Sci. Technol. **48**, 968 (2005).

[4]C. T. Holcomb, M. A. Makowski, S. L. Allen, W. H. Meyer, and M. A. Van Zeeland, Rev. Sci. Instrum. **79**, 10F518 (2008).

[5]A. Malaquias, M. von Hellermann, S. Tugarinov, P. Lotte, N. Hawkes, M. Kuldkepp, E. Rachlew, A. Gorshkov, C. Walker, A. Costley, and G. Vayakis, Rev. Sci. Instrum. **75**, 3393 (2004).

[6]C. T. Holcomb, S. L. Allen, M. A. Makowski, R. J. Jayakumar, M. F. Gu, S. Lerner, K. L. Morris, J. Latkowski, J. M. Moller, W. Meyer, R. Ellis, R. Geer, D. Behne, R. Chipman, P. Smith, and S. McClain, "An overview of the motional Stark effect diagnostic on DIII-D and design work for an ITER MSE," Burning Plasma Diagnostics: An International Conference (AIP Conf. Proc. 2008) Vol. 988, p. 214.

[7]N. A. Pablant, K. H. Burrell, R. J. Groebner, D. H. Kaplan, and C. T. Holcomb, Rev. Sci. Instrum. **79**, 10F517 (2008).

[8]K. Jakubowska, M. De Bock, R. Jaspers, M. G. von Hellermann, and L. Shmaenok, Rev. Sci. Instrum. **75**, 3475 (2004).

[9]W. Mandl, R. C. Wolf, M. G. von Hellermann, and H. P. Summers, Plasma Phys. Control. Fusion **35**, 1373 (1993).

[10]R. J. E. Jaspers, M. G. von Hellermann, E. Delabie, W. Biel, O. Marchuk, and L. Yao, Rev. Sci. Instrum. **79**, 10F526 (2008).

[11]R. Wolf, L. Eriksson, M. Hellermann, R. Koenig, W. Mandl, and F. Porcelli, Nucl. Fusion **33**, 1835 (1993).

[12]D. J. D. Hartog, D. Craig, D. A. Ennis, G. Fiksel, S. Gangadhara, D. J. Holly, J. C. Reardon, V. I. Davydenko, A. A. Ivanov, A. A. Lizunov, M. G. O'Mullane, and H. P. Summers, Rev. Sci. Instrum. **77**, 10F122 (2006).

13B. W. Rice, K. H. Burrell, L. L. Lao, and Y. R. Lin-Liu, Phys. Rev. Lett. 79, 2694 (1997).

[14]B. H. Bransden and C. Joachain, *Physics of Atoms and Molecules*, 2nd ed. (Prentice Hall, Upper Saddle River, NJ, 2003).

[15]D. M. Thomas, K. H. Burrell, R. J. Groebner, P. Gohil, D. Kaplan, C. Makariou, and R. P. Seraydarian, Rev. Sci. Instrum. **68**, 1233 (1997).

[16]H. Chiu, Fusion Sci. Technol. **34**, 564 (1998).

[17]R. P. Seraydarian, K. H. Burrell, N. H. Brooks, R. J. Groebner, and C. Kahn, Rev. Sci. Instrum. **57**, 155 (1986).

[18]M. G. von Hellermann, E. Delabie, R. Jaspers, P. Lotte, and H. P. Summers, Spectral Line Shapes: Vol. 15, 19th International Conference on Spectral Line Shapes, AIP Conf. Proc., 1058, 187 (2008).

[19]B. W. Rice, K. H. Burrell, and L. L. Lao, Nucl. Fusion **37**, 517 (1997).

## ACKNOWLEDGMENT

This work was partially supported by the U.S. Department of Energy under DE-FC02-04ER54698, DE-FG02-07ER54917 and DE-AC52-07ER27344.